

Vesicles and actin are targeted to the cleavage furrow via furrow microtubules and the central spindle

Roger Albertson, Jian Cao, Tao-shih Hsieh, and William Sullivan

Department of Molecular, Cellular, and Developmental Biology, University of California, Santa Cruz, Santa Cruz, CA 95064

During cytokinesis, cleavage furrow invagination requires an actomyosin-based contractile ring and addition of new membrane. Little is known about how this actin and membrane traffic to the cleavage furrow. We address this through live analysis of fluorescently tagged vesicles in postcellularized *Drosophila melanogaster* embryos. We find that during cytokinesis, F-actin and membrane are targeted as a unit to invaginating furrows through formation of F-actin-associated vesicles. F-actin puncta strongly colocalize with endosomal, but not Golgi-derived, vesicles. These vesicles are recruited

to the cleavage furrow along the central spindle and a distinct population of microtubules (MTs) in contact with the leading furrow edge (furrow MTs). We find that Rho-specific guanine nucleotide exchange factor mutants, *pebble* (*pbl*), severely disrupt this F-actin-associated vesicle transport. These transport defects are a consequence of the *pbl* mutants' inability to properly form furrow MTs and the central spindle. Transport of F-actin-associated vesicles on furrow MTs and the central spindle is thus an important mechanism by which actin and membrane are delivered to the cleavage furrow.

Introduction

During the last several years, studies from a variety of systems have revealed that membrane trafficking events play an important role during animal cytokinesis (Strickland and Burgess, 2004; Albertson et al., 2005; Otegui et al., 2005). For example, disrupting exocytic, endocytic, or recycling pathways by drug inhibition or mutations often causes abnormal regression of cleavage furrows (Schweitzer and D'Souza-Schorey, 2004). Likewise, proteins involved in vesicle transport, such as Syntaxin, are localized to furrows and necessary for furrow ingression (Burgess et al., 1997; Finger and White, 2002; Schweitzer and D'Souza-Schorey, 2004). In addition, three comprehensive RNAi screens in *Caenorhabditis elegans* and *D. melanogaster* S2 cells have each identified a significant number of membrane trafficking genes necessary for cytokinesis (Echard et al., 2004; Eggert et al., 2004; Skop et al., 2004). Considering that three independent screens in different systems all identified membrane trafficking genes highlights the general importance of this process in animal cytokinesis.

In dividing cells, actin accumulation to furrows is thought to occur early during cytokinesis, yet little is known mechanistically about how actin is recruited. In mammalian cell culture, it has been reported that cortical actin filaments from polar regions are redistributed to the equatorial cell cortex during early anaphase (Cao and Wang, 1990b). In contrast, other studies suggest that actin and membrane delivery to furrows is coordinated through a membrane trafficking pathway. In the early *D. melanogaster* embryo, mutations in *nuf* and *rab11* cause disorganized recycling endosomes (RE), which compromise both membrane and actin organization at furrows (Rothwell et al., 1999; Riggs et al., 2003). Similarly, in *C. elegans* and mammalian cell culture, Rab11 activity and a functional RE are required during late cytokinesis stages, which is consistent with a role for the recycling pathway in vesicle-based membrane and actin delivery to furrows (Skop et al., 2001; Wilson et al., 2005). Other studies have provided evidence linking plasma membrane composition to actin reorganization during cytokinesis. In several systems, the lipid phosphatidylinositol has been shown to coordinate plasma membrane and F-actin organization at the cleavage furrow (Logan and Mandato, 2006). Also, membrane delivery has been linked to actin organization at the furrow. In *D. melanogaster* embryos, disrupting a core regulator of vesicle fusion, Syntaxin1, disrupts actin reorganization during furrow formation (Burgess et al., 1997).

Correspondence to William Sullivan: sullivan@biology.ucsc.edu

Abbreviations used in this paper: Dlg, discs large; MT, microtubule; NRK, normal rat kidney; n-Syb, n-synaptobrevin; RE, recycling endosomes; Syt, synaptotagmin; WT, wild type.

The online version of this paper contains supplemental material.

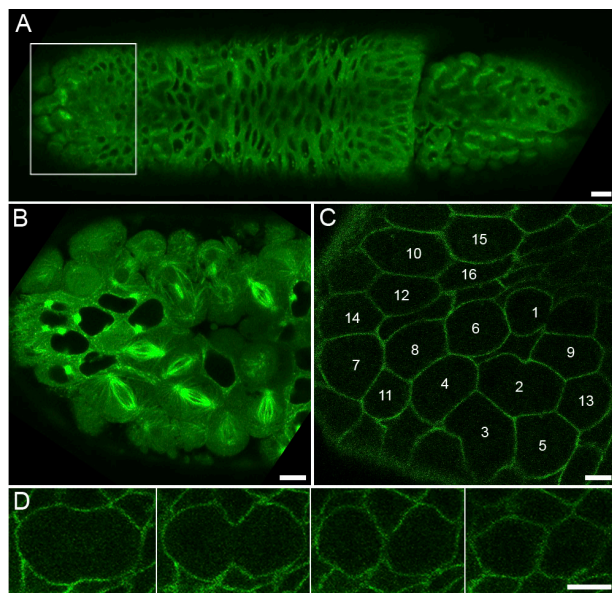


Figure 1. **Live imaging of cycle 14 mitotic domains.** (A) Tubulin-GFP. Dividing cells are clustered in mitotic domains (box). (B) Magnification of box in A. (C) Dlg-GFP. Cells within a mitotic domain enter mitosis as a cluster and divide in a characteristic order. (D) Dlg-GFP is uniform cortical during cytokinesis. Bars: (A) 10 μ m; (B–D) 5 μ m.

The central spindle plays a prominent role in the proper formation and ingression of cleavage furrows in most animals (for reviews see Gatti et al., 2000; D'Avino et al., 2005). Its assembly requires a conserved centralspindlin complex, consisting of MKLP1 kinesin and RacGAP. Loss of either component causes a partial to complete loss of central spindle formation and a subsequent failure in cleavage furrow formation (*D. melanogaster*) or ingression (*C. elegans* and mammals). RacGAP and Rho-specific guanine nucleotide exchange factor activity at the central spindle is thought to provide a signal for RhoA-mediated F-actin reorganization and contractile ring assembly at the furrow, subsequently stimulating ingression (for review see D'Avino et al., 2005). It is likely that a variety of proteins at the central spindle contribute to multiple aspects of cytokinesis, although relatively few furrow-promoting proteins have been analyzed. A recent mass spectrometry screen to characterize central spindle components found four main protein categories: secretory and membrane associated (33%), actin associated (29%), microtubule (MT) associated (11%), and kinases (11%; Skop et al., 2004). Our current knowledge indicates that central spindle function likely involves both direct signaling to the cleavage furrow and regulation of membrane traffic events, although the emphasis placed upon specific roles varies among organisms. In this paper, we present evidence for a model in which F-actin-associated vesicles rely on the central spindle and specialized furrow MTs for transport to the cleavage furrow.

Results

To study the roles of furrow MTs, the central spindle, and membrane traffic in cytokinesis, we have used the first conventional division immediately after cellularization in *D. melanogaster*

embryos (Foe, 1989). After cellularization, cycle 14 cells form mitotic domains, which are clusters of cells united by locally synchronous mitosis (Fig. 1 A, box). Cells have a large size and divide at the surface of the embryo, making high-resolution live fluorescent analysis straightforward (Fig. 1 B). Within each cluster, mitosis begins with a single cell and then spreads across neighboring cells to the domain boundary (Fig. 1 C). GFP fusion proteins can be used to monitor cleavage furrow morphology and ingression as well as membrane trafficking components. For example, discs large (Dlg) is a cortical scaffolding protein (Bilder et al., 2000) and Dlg-GFP shows uniform cortical localization throughout the cell cycle (Fig. 1 C) and cytokinesis (Fig. 1 D). The majority of images in this study were obtained using GFP fusion proteins and rhodamine-labeled tubulin or actin (see Materials and methods).

GFP-tagged vesicles are targeted to cleavage furrows

To visualize vesicle transport in dividing cells, two Gal4-driven GFP-tagged vesicle markers were expressed: synaptotagmin (Syt) and n-synaptobrevin (n-Syb; Zhang et al., 2002). Syt and n-Syb are integral synaptic vesicle proteins. Syt functions in Ca^{2+} -mediated exocytosis at nerve terminals (Tucker and Chapman, 2002), whereas n-Syb is a neuron-specific V-SNARE (Deitcher et al., 1998). Syt-GFP and n-Syb-GFP have both been shown to label synaptic vesicles (Estes et al., 2000; Zhang et al., 2002). In this paper, we use Syt-GFP and n-Syb-GFP as new markers for vesicular structures in dividing cells. During cycle 14, both Syt-GFP and n-Syb-GFP were localized to punctate structures throughout all cells examined. From interphase to anaphase, Syt-GFP showed a uniform distribution at the plasma membrane as well as cytoplasmic puncta (unpublished data). Midway through cleavage furrow invagination, GFP-tagged puncta were seen at the cell equator and strongly enriched at furrows, which persisted several minutes after scission (Fig. 2 A, arrowheads and arrows; and Video 1, available at <http://www.jcb.org/cgi/content/full/jcb.200803096/DC1>). In particular, individual puncta were seen moving toward, and embedding into, the furrow (Fig. 2 A, arrows). Similarly, n-Syb-GFP-labeled vesicles showed strong enrichment at mid-to-late stages of furrow ingression (Fig. 2 B, arrowhead), indicating that vesicle enrichment is not peculiar to the Syt-GFP marker. In addition to cycle 14 cells, this localization pattern is common for a variety of dividing cell types, including epithelia and neuroblast cells during later embryonic stages (Fig. S1, available at <http://www.jcb.org/cgi/content/full/jcb.200803096/DC1>). Therefore, given the punctate labeling and dynamic behavior shown in dividing cells, these puncta are regarded as representing vesicles from an as yet unidentified source.

The GFP signal increase at furrows could have two sources: GFP-tagged proteins at the plasma membrane may become concentrated at cleavage furrows during telophase and/or GFP-tagged vesicles in the cytoplasm may get targeted to furrows. Two observations indicate that a portion of the GFP enrichment at furrows is derived from vesicles. Monitoring individual Syt-GFP puncta showed movement toward ingressing furrows, where puncta subsequently became embedded into

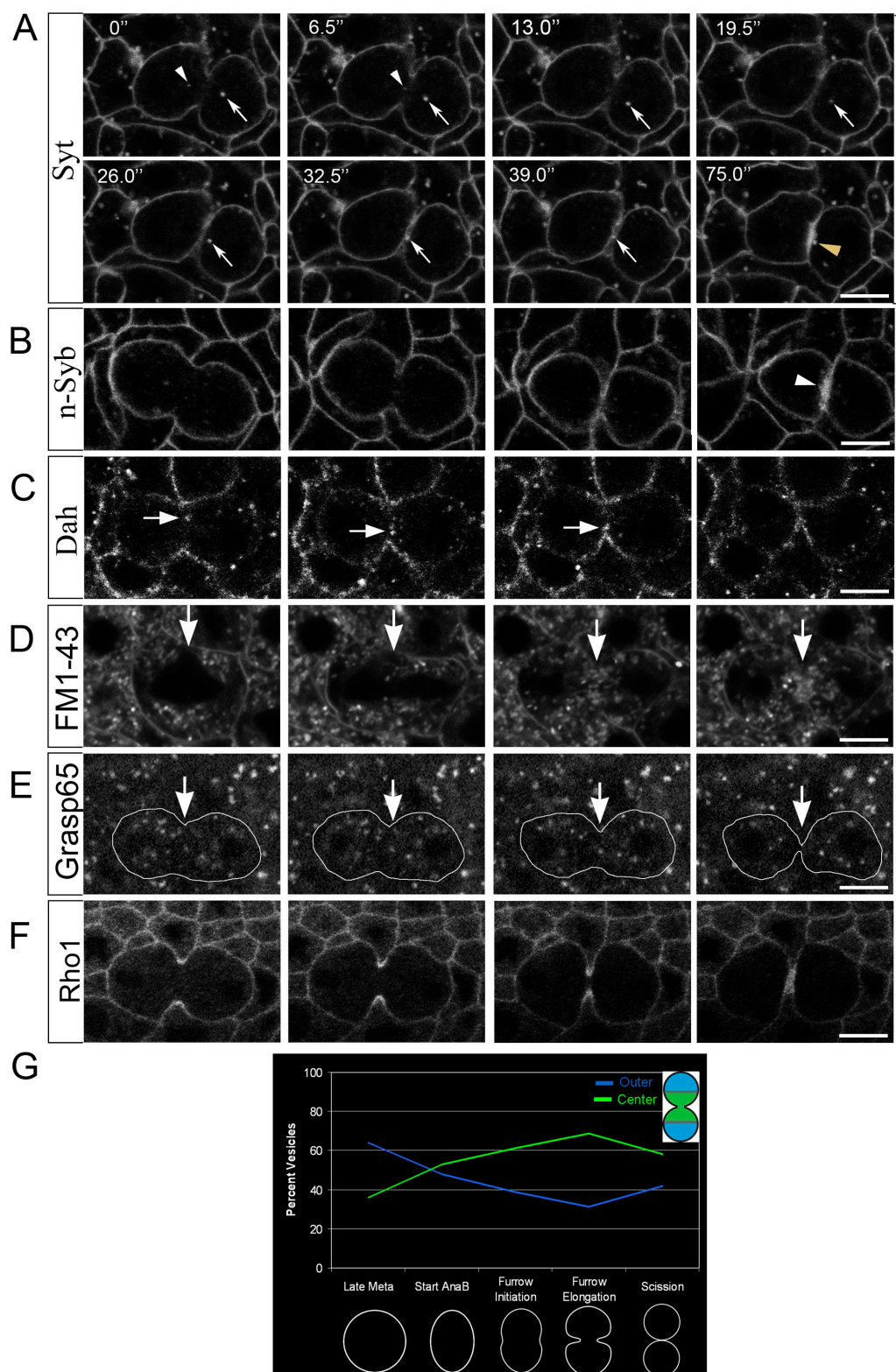
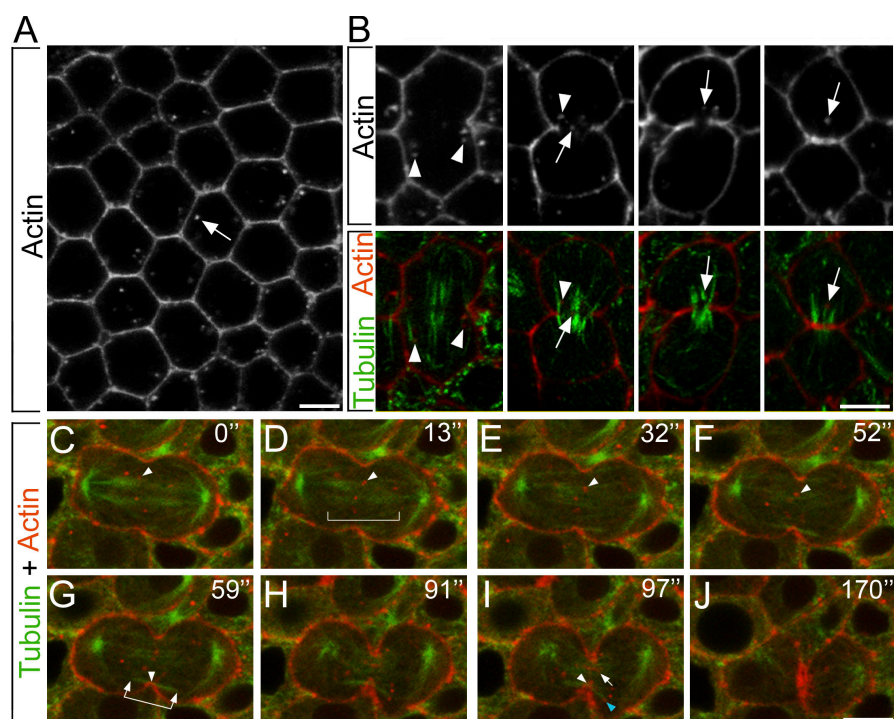


Figure 2. Vesicles and membrane are targeted to furrows during cytokinesis in cycle 14 cells. All images are from living embryos. (A) Syt-GFP-labeled vesicles. Arrows indicate a single vesicle. Arrowheads indicate other vesicles moving toward the furrow. Time points (s) are shown at the top left of each panel. For the full video, see Video 1, available at <http://www.jcb.org/cgi/content/full/jcb.200803096/DC1>. (B) n-Syb-GFP-labeled vesicles show strong furrow enrichment at cytokinesis (arrowhead). (C) Dah-GFP vesicles show cytoplasmic puncta at the cell equator and furrow enrichment at cytokinesis (arrows). (D) The general membrane dye FM1-43 accumulates at the cell equator during cytokinesis. Arrows, cleavage plane. (E) Grasp-65-GFP-labeled Golgi do not accumulate at the cell equator at cytokinesis. Arrows, cleavage plane. Outline, cell cortex. (F) RhoA-GFP. (G) Percentage of vesicles localized to polar regions of the cell (outer) and to the middle of the cell (center). Cells were divided into thirds (inset). Vesicle localization was scored at cell stages indicated on the x axis. $n = 92$ (late metaphase), 74 (anaphase B), 96 (furrow initiation), 91 (elongation), or 100 (scission). Bars, 5 μm .

Figure 3. Actin puncta are targeted to ingressing furrows. (A) Phalloidin in fixed embryos shows F-actin puncta in cycle 14 interphase cells (arrow). (B) F-actin puncta localize to the cell equator near furrow MTs (arrowheads) and the central spindle at cytokinesis (arrows). Merged images of F-actin (phalloidin; red) and MTs (α -Tub; green) are shown in the bottom panels. (C–J) Live series of cycle 14 telophase. Rhodamine-actin, red; Tub-GFP, green. Actin puncta accumulate near the central spindle (D, bracket). Arrowheads in C–F show an individual actin puncta moving alongside an MT bundle at the central spindle. Furrow MTs (G, arrowed bracket) align perpendicular to the cleavage plane. Its midpoint contacts the furrow tip (G, arrowhead). Actin puncta are visible near ends of furrow MTs (I, blue arrowhead) and accumulate at the contact point between the leading furrow edge and furrow MTs (G and I, white arrowheads). Arrow in I shows an actin puncta colocalized with the central spindle. Time points (s) are shown at the top right of each panel. For full video, see Video 2, available at <http://www.jcb.org/cgi/content/full/jcb.200803096/DC1>. Bars, 5 μ m.



furrows (Fig. 2 A, arrows). Second, monitoring populations of Syt-GFP puncta demonstrates accumulation of puncta at the cell equator during mitosis, with a peak during furrow elongation (Fig. 2 G). Other GFP markers remained uniformly distributed along the cortex before and during cytokinesis (Fig. 1 D, Dlg-GFP). This indicates that increases in Syt- and n-Syb-GFP signal intensities at furrows is not merely caused by the combined fluorescence of multiple plasma membrane surfaces entering the same focal plane during late cytokinesis.

To further investigate if vesicle transport to furrows is a general process in dividing cells, we examined the distribution of the *D. melanogaster* dystrophin homologue Dah, a vesicle-associated component that is normally expressed during early embryogenesis (Rothwell et al., 1999). During cytokinesis in cycle 14 cells, Dah-GFP-marked vesicles were observed near ingressing furrows and enriched at the furrow membrane (Fig. 2 C, arrows). We next monitored internal cell membranes during mitosis by injecting the general membrane dye FM1-43 (Fig. 2 D). During cytokinesis, membrane structures became enriched at the cell equator, supporting the idea that considerable membrane traffic is directed toward ingressing furrows. In contrast, Grasp65-labeled Golgi were randomly distributed during cytokinesis, indicating that not all types of vesicles are targeted to the cell equator (Fig. 2 E). Because Rho family proteins have been implicated in membrane traffic (Ridley, 2006), we examined the localization of RhoA, a known contractile ring component. RhoA-GFP showed strong enrichment at the leading furrow edge but showed no localization to cytoplasmic membrane structures (Fig. 2 F), demonstrating that not all furrow components are enriched through vesicle-based delivery. Collectively, the data indicate that a subset of vesicles is targeted to ingressing furrows during cytokinesis.

Cytoplasmic F-actin delivery to furrows occurs midway through furrow invagination

During cell division, F-actin transport to furrows is thought to occur during early cytokinesis, yet the mechanism underlying actin recruitment to furrows remains unclear. One model proposes the redistribution of cortical actin filaments (Cao and Wang, 1990b), whereas a second model proposes vesicle-based actin delivery (Riggs et al., 2003). To investigate this further, F-actin localization was examined in fixed embryos. Phalloidin staining of cycle 14 interphase cells showed uniform cortical F-actin as well as F-actin puncta in the cytoplasm (Fig. 3 A, arrow). During early-to-mid cytokinesis stages, F-actin puncta became enriched at the cell equator near furrow MTs and the central spindle (Fig. 3 B). During mid-to-late cytokinesis, F-actin became highly enriched at furrows (Fig. 3 B). These results suggest that F-actin puncta become enriched at the furrow analogous to Syt, n-Syb, and Dah vesicle markers.

To simultaneously monitor actin transport relative to the mitotic spindle, fluorescently labeled actin was injected into embryos expressing Tubulin-GFP. Live imaging revealed that actin puncta localize to and move alongside of midzone MTs during telophase (Fig. 3, C–F, arrowheads [bracket in D marks midzone]; and Video 2, available at <http://www.jcb.org/cgi/content/full/jcb.200803096/DC1>). Actin puncta accumulation at the cell equator continues through late telophase (Fig. 3, G–J), during which puncta colocalize with the central spindle (Fig. 3 I, arrow). In addition to central spindle MTs, distinct bundles of furrow MTs (Fig. 3 G, arrowed bracket) aligned perpendicular to the cleavage plane, with their midpoint contacting the leading furrow edge (Fig. 3 G, arrowhead; and see also Fig. 6 O). Actin puncta were observed near the distal region of furrow MTs (Fig. 3 I, blue arrowhead) and accumulated at the contact point between the leading furrow edge and furrow MTs (Fig. 3, G and I,

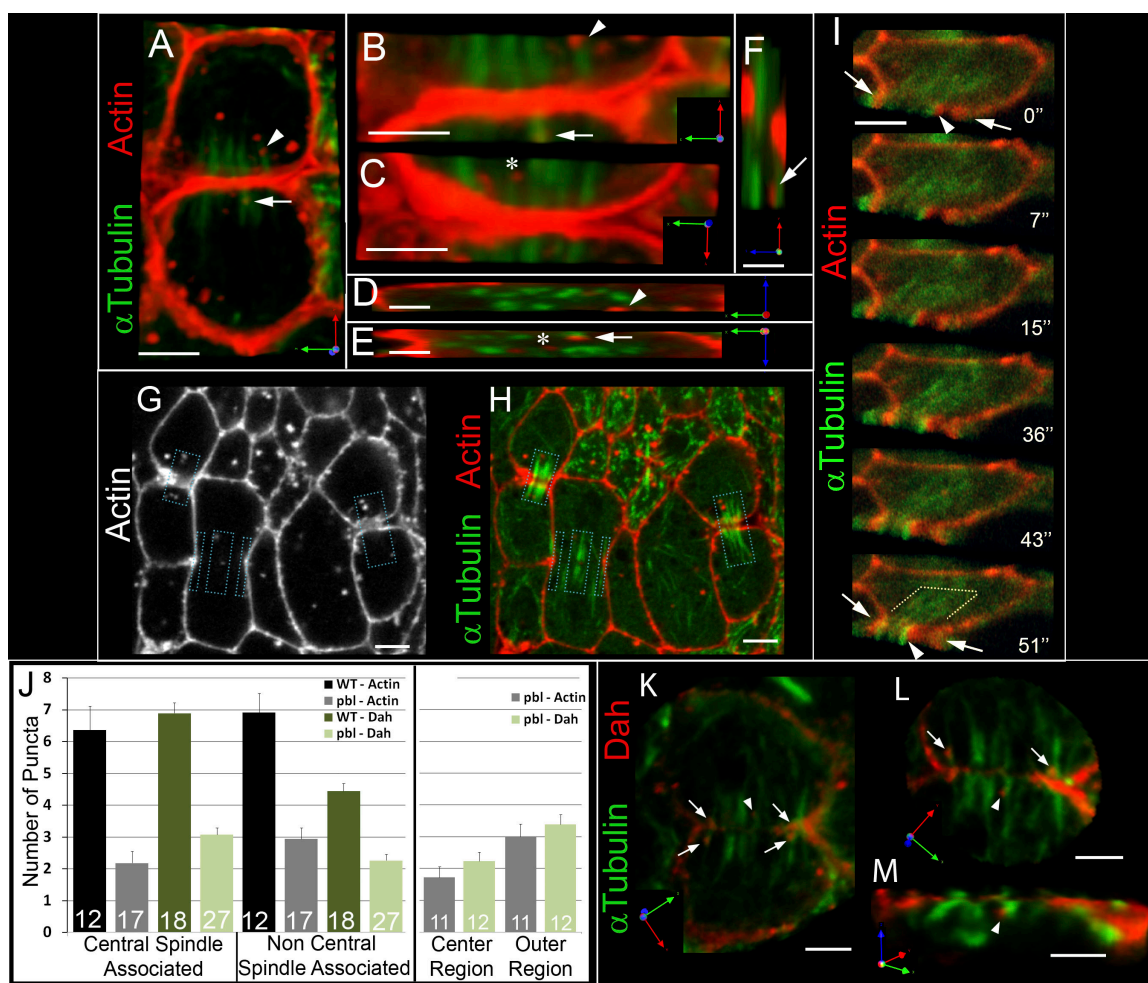


Figure 4. 3D imaging of actin and vesicles. Markers are shown to the left of panels. 3D perspective is indicated at the bottom right panel corners. (A–H) Phalloidin in fixed embryos. Arrows, arrowheads, and asterisks show individual actin puncta that correspond in each rotation (A–F). (G and H) Boxes show the region considered the central spindle for quantifications. (I) Live series of α -Tub and rhodamine-actin. Time points (s) are indicated at the bottom right of each panel. Images were cropped at the furrow (arrows) and rotated 45° to show xy and z planes. Arrowheads indicate actin puncta colocalized with MT bundle. Dotted bracket indicates central spindle. (J) Genotypes and markers are shown at the top right and cell number (n) is shown in bars. Error = SEM. Center region in the right graph includes the middle one-third of the cell in the xy plane. (K and L) Dah-positive vesicles localize to furrow MTs (arrows) and central spindle MTs (arrowheads). Arrows and arrowheads correspond to same vesicle in each rotation (L and M). Step size = 150 nm, except I (200 nm). Bars: (A and G–L) 3 μ m; (B, C, and M) 2 μ m; (D–F) 1 μ m.

white arrowheads), where they appeared to incorporate into the furrow. Subsequently, actin became highly enriched in furrows during the final stage of cytokinesis (Fig. 3 J). This suggests that delivery of actin puncta to the furrow relies on directed transport along MTs that is similar to vesicle-based transport.

Cytoplasmic actin delivery to furrows utilizes vesicles, central spindle, and furrow MTs

To further investigate the relationship between actin puncta and MT bundles, 3D imaging was performed in both fixed and living embryos. To maximize the resolution in the z plane, very thin sections (between 150 and 200 nm) were acquired. In fixed embryos, a population of actin puncta accumulated at the central spindle (Fig. 4 A) and was seen in close proximity to MT bundles in the xy plane (Fig. 4, A–C, arrow, arrowhead, and asterisk; and Video 3, available at <http://www.jcb.org/cgi/content/full/jcb.200803096/DC1>). Image stack rotations, showing the

z plane, revealed actin puncta in very close proximity (often within ~ 200 nm) to individual MT bundles of the central spindle and furrow MTs (Fig. 4, D [arrowhead], E [asterisk and arrow], and F [arrow]). Furthermore, 3D imaging in living embryos revealed colocalization between actin puncta and MT bundles adjacent to the ingressing furrow (Fig. 4 I). These puncta were distinct from the furrow (Fig. 4 I, arrowhead and arrows, respectively), remained localized at a central spindle bundle through telophase, and appeared to integrate with the furrow during mid to late cytokinesis (Fig. 4 I, 51").

To quantify the portion of actin puncta localized at the central spindle, puncta localization was scored in a 3- μ m-thick section per cell (the approximate depth of the central spindle). The central spindle occupied a relatively small region of the volume examined (Fig. 4, G and H, boxes), yet about half of the actin puncta are localized at the central spindle ($47.5 \pm 1.9\%$; Fig. 4, H and J). This observation is consistent with 2D imaging that showed an accumulation of actin puncta at the central spindle.

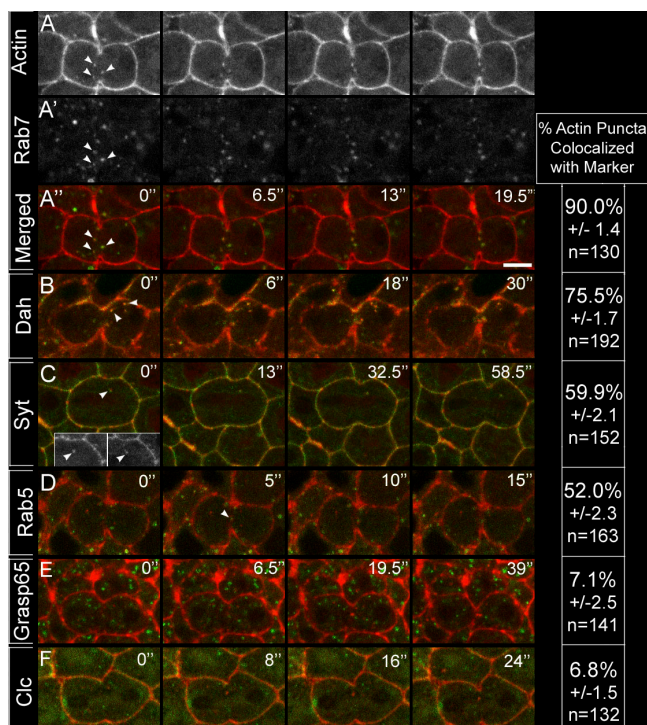


Figure 5. Live imaging shows that actin puncta associate with vesicles and endosomes. Rhodamine-actin (red) was injected into embryos expressing a distinct GFP fusion protein (green; specified in left column). Puncta was scored as colocalized if two puncta moved in unison over a minimum of two consecutive time points (arrowheads). Time points (s) are indicated at the top right of panel. Percentage of colocalization is shown in the right column. (A–F) Live series shows that actin puncta colocalize with Rab7-GFP-labeled late endosomes (A), Dah-GFP-labeled vesicles (B), Syt-GFP-labeled vesicles (C), and Rab5-GFP-labeled early endosomes (D). Actin puncta did not show considerable colocalization with Grasp65-GFP-labeled Golgi (E) or Clathrin light chain-GFP-labeled membrane (F). Insets in C depict single channels for actin (left) and Syt-GFP (right). Error = SEM. Bar, 5 μ m

Vesicle and MT colocalization was further examined with the vesicle marker Dah. Similar to actin puncta dynamics, 3D imaging revealed an accumulation of Dah-labeled vesicles in close proximity to furrow MTs (Fig. 4, K and L, arrows; and Video 4, available at <http://www.jcb.org/cgi/content/full/jcb.200803096/DC1>) and central spindle MT bundles (Fig. 4, K–M, arrowheads) in both xy and z planes. Quantification of vesicle localization within a 3- μ m depth showed that a majority of vesicles ($61 \pm 2.8\%$; $n = 204$ vesicles in 18 cells) are closely localized to central spindle MT bundles (Fig. 4 J). Collectively, these data support the notion that F-actin puncta and Dah-associated vesicles are targeted toward ingressing furrows via central spindle and furrow MTs during cytokinesis.

F-actin puncta are primarily associated with endosome-derived vesicles

Our observations that actin puncta show a similar localization pattern to vesicle markers during cycle 14 mitosis is consistent with reports of vesicle-associated actin in other systems (Riggs et al., 2003; Fernandez-Borja et al., 2005; Ridley, 2006). We therefore sought to identify if actin puncta are vesicle-associated in cycle 14 cells and to determine what specific vesicle subpop-

ulations actin may be associating. To do so, actin localization was compared with various membrane trafficking components, each specific to a vesicle subpopulation. Rhodamine-actin was injected into a series of embryos, each expressing a unique GFP-tagged membrane marker (Fig. 5). We then assayed for puncta colocalization, designating puncta that moved in unison over at least two time points (≤ 6.5 s) as “colocalized” (Fig. 5, arrowheads; $n > 125$ actin puncta for each assay). Actin puncta were highly associated with Rab7-marked late endosomes (90% colocalization; Fig. 5, arrowheads) as well as with Dah- and Syt-marked vesicles (75.5 and 59.9% colocalization, respectively). A moderate portion of actin puncta associated with Rab5-marked early endosomes (52%). In contrast, actin puncta were not found to associate with Grasp65-GFP-marked Golgi (7.1%) or clathrin light chain-labeled puncta (6.8%). Collectively, these results indicate that cytoplasmic actin transport involves an endosome-derived vesicle-based mechanism, rather than a Golgi-based secretory pathway.

Pbl is necessary for vesicle and actin recruitment to the cell equator

In genetic screens designed to identify genes involved in cytokinesis and vesicle recruitment to the furrow (unpublished data), we found vesicle and actin transport defects in Rho-specific guanine nucleotide exchange factor *pbl* mutants. Wild-type (WT) embryos show crisp Syt-GFP localization at the cell cortex and vesicles. In contrast, zygotic *pbl*^Δ mutants showed weak and diffuse Syt-GFP at the cell cortex and cytoplasm (Fig. 6, A–C; and Videos 5, 6, and 7, available at <http://www.jcb.org/cgi/content/full/jcb.200803096/DC1>), which is indicative of defects in vesicle transport. In particular, very few *Pbl*-deficient cells showed Syt-GFP-positive vesicle accumulation at the cell equator (9% [$n = 24$] in *pbl*^Δ vs. 100% [$n = 30$] in WT), and furrows lacked vesicle enrichment, even in cells with full furrow elongation (Fig. 6 C and Video 7). We also examined actin localization in *pbl*^Δ embryos. During early telophase in WT embryos, actin was uniform cortical and associated with robust puncta. At late telophase actin became strongly enriched at furrows (Fig. 6 D and Video 5). In *pbl*^Δ embryos, actin was diffusely localized at the cell cortex and puncta (Fig. 6, E and F). During telophase, *pbl*^Δ showed reduced actin puncta localization to the cell equator, particularly in cells that are unable to furrow (Fig. 6, E and F; and Videos 6 and 7). Collectively, these data indicate that *Pbl* function is important for proper vesicle and actin puncta recruitment to the cell equator during telophase.

Pbl is necessary for proper furrow MT formation

It has previously been reported that *Pbl* function is necessary for central spindle integrity (Prokopenko et al., 1999). Because we observed actin puncta colocalized with the central spindle in WT embryos, we took advantage of *pbl* mutants to investigate whether actin puncta recruitment is dependent on the central spindle (see next section). These assays revealed an unexpected role for *Pbl* in the formation of furrow MTs during very early cytokinesis. In this paper, we compare furrow MT

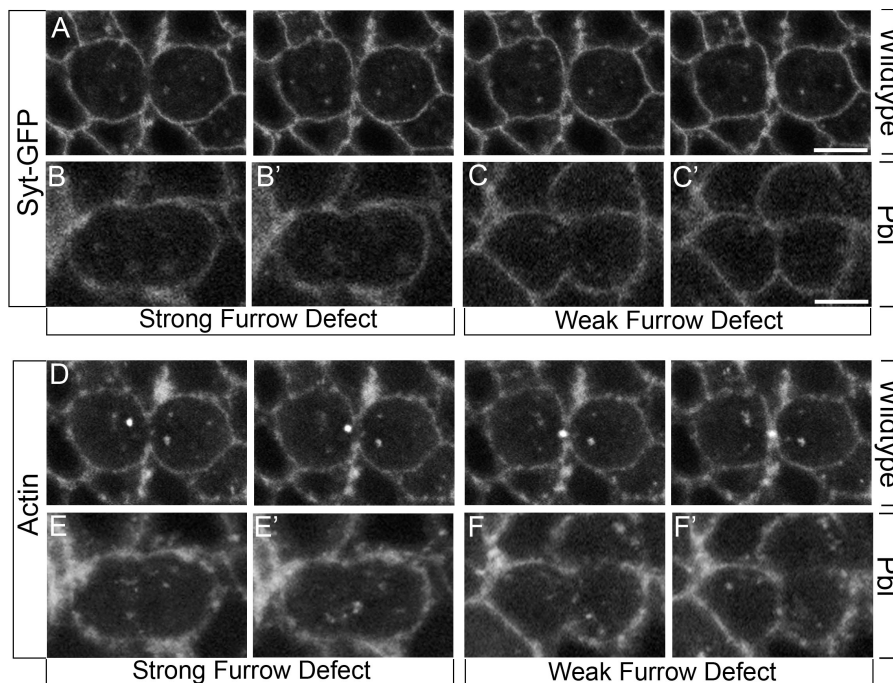


Figure 6. *pbl* embryos have defects in vesicle transport. Markers are indicated on the left. Genotypes are indicated on the right. All panels show live images. (A–F) Actin and Syt-GFP vesicles strongly localize to furrows during cytokinesis in WT (A and D). *pbl* embryos fail to localize Syt-GFP vesicles to the cell equator in cells with severe furrowing defects (B) and cells with weak furrowing defects (C). *pbl* embryos show weak actin recruitment to the cell equator (E and F). The furthest extent of furrow elongation is shown in B', C', E', and F'. For full videos, see Videos 5, 6, and 7, available at <http://www.jcb.org/cgi/content/full/jcb.200803096/DC1>. Bars, 5 μ m.

dynamics in WT (Fig. 7, A–F) and *pbl*² embryos (Fig. 7, G–L), relative to cell cycle progression and furrow elongation (Fig. 7, A'–L' and M).

In WT embryos, the metaphase spindle (Fig. 7 A) is reorganized to form midzone MTs at anaphase (Fig. 7 B), which condense into a tightly packed central spindle during telophase (Fig. 7, C and D). The central spindle is maintained after the completion of furrow invagination (Fig. 7 E), leading to daughter cells with a single nucleus (Fig. 7 F). A distinct intensely staining MT bundle is also visible perpendicular to the furrow during early telophase (Fig. 7, O and O'). The midpoint of these furrow MTs contacts the leading edge of the furrow and remains in front of the furrow throughout invagination (Fig. 7, O and O', arrowheads). Furrow MTs appear to be connected to the central spindle through several thin MT bundles (Fig. 7 O, arrows). During late telophase, furrow MTs integrate with the central spindle (Fig. 7 D), forming a massive collection of MTs.

Consistent with previous reports of ECT2/Pbl (Hime and Saint, 1992; Lehner, 1992; Prokopenko et al., 1999; Tatsumoto et al., 1999; Echard and O'Farrell, 2003; Morita et al., 2005), zygotic-null *pbl* mutants failed furrow invagination, showed disrupted central spindle integrity, and accumulated binucleate cells (Fig. 7, K' and L'). In addition, we observed early furrow MT defects not previously described for *pbl* mutations. Mitotic stages in *pbl*² embryos can be easily identified because chromosome segregation during anaphase is normal and cells exhibit typical telophase nuclei in which chromosomes fully decondense (Fig. 7, H'–K'). During telophase, *pbl*² embryos differed substantially from the WT (Fig. 7, C'–E') in that they lacked organized furrow MT bundles and failed central spindle maintenance. Compared with the WT, *pbl*² embryos showed weak central spindle formation at early telophase (17.9 [WT] vs. 44.4% [*pbl*²]; Fig. 7, I, M, and P), had a severe

loss of central spindle maintenance by late telophase (0 [WT] vs. 66.7% [*pbl*²]; Fig. 7, J and M), and lacked a central spindle at the end of telophase (0 [WT] vs. 100% [*pbl*²]; Fig. 7, K and M). Furthermore, *pbl*² embryos either lacked or showed poorly formed furrow MTs at early telophase (Fig. 7, compare O to P, arrowheads, and Q, quantification). The onset of furrow MT defects preceded that of central spindle defects (Fig. 7, compare early telophase in M to Q). We note that a small minority of cells in *pbl*² embryos were able to form weak furrows that fully invaginated yet had a completely disorganized central spindle (Fig. 7 N).

This data suggest that Pbl is required for normal furrow MT formation and maintenance. Significantly, Prokopenko et al. (1999) describe punctate Pbl localization at the leading furrow edge (in addition to nuclear Pbl). A very similar Pbl localization pattern of nuclear and punctate staining was evident in cycle 14 cells (Fig. 7 R). Simultaneous labeling of the cell cortex (anti-Scribble) and the mitotic spindle (anti- α -tubulin) revealed Pbl puncta at the contact point between furrow MTs and the leading furrow edge (Fig. 7 R, arrows). Specifically, Pbl showed clear association with furrow MTs (e.g., Fig. 7 R, right arrow). Collectively, the Pbl protein distribution and the *pbl* spindle phenotype suggest that, in addition to its known role in maintaining the central spindle, Pbl plays a role in furrow MT formation and maintenance.

Furrow MT and central spindle maintenance is an important factor in actin delivery to the cleavage plane

Given the observations of furrow MT and central spindle defects in fixed *pbl* embryos (Fig. 7), we further examined MT dynamics in living *pbl* embryos, with particular focus on furrow MT, central spindle maintenance, and actin puncta localization. In WT cells at early telophase, furrow MTs form

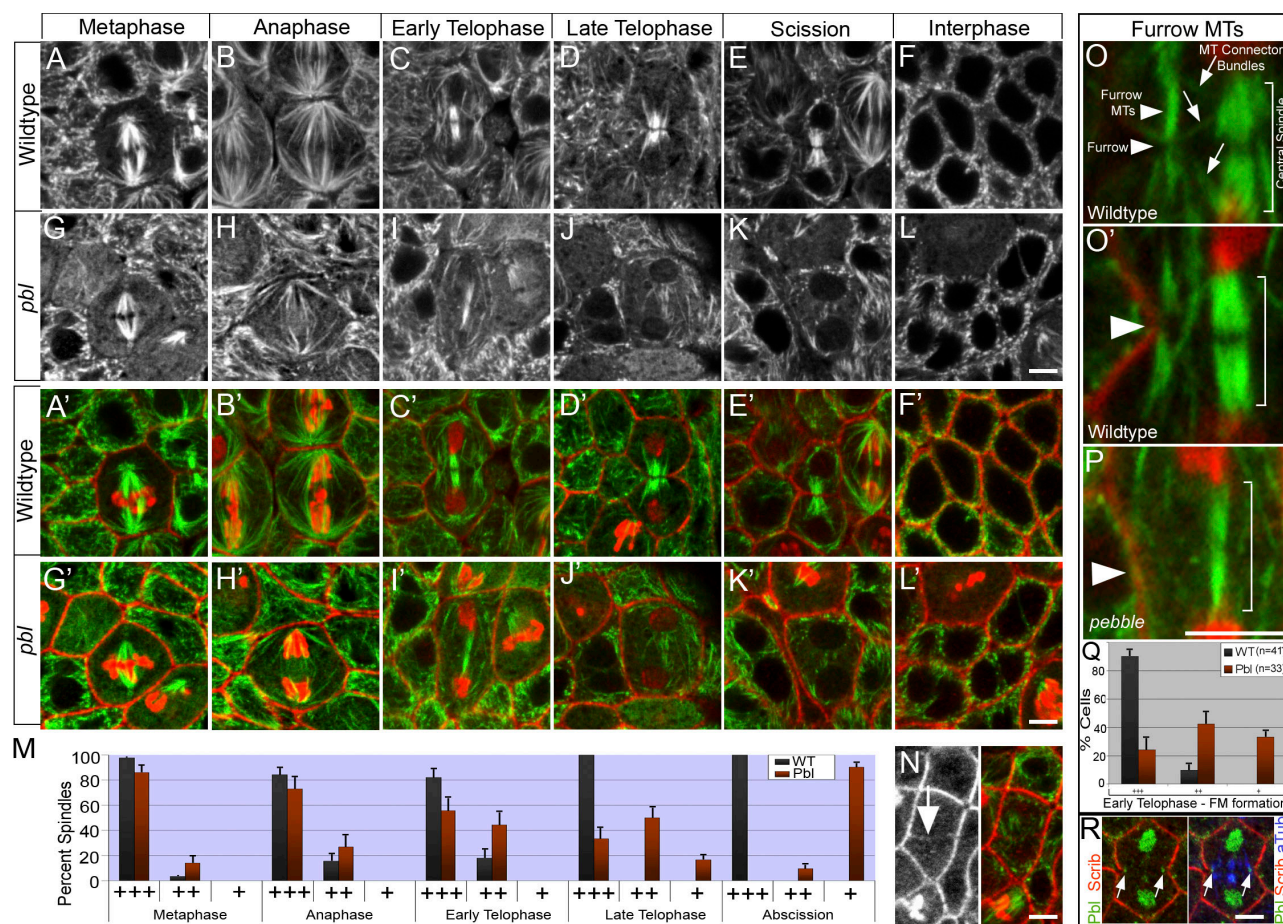


Figure 7. *pbl* mutants have defects in furrow MT and central spindle organization. All panels show fixed embryos. green, α -tubulin and slight γ -tubulin; red, PH3 and Scribble (for all stains except R [green, Pbl; blue, α -tubulin]). (A–L) WT (A–F) and *pbl*² (G–L) from cycle 14 metaphase (A and G) through cycle 15 interphase (F and L). (A'–L') Merged images correspond to A–L. (M) Percentage of normal (+++), weak (++), and severely disrupted (+) spindles at various stages in WT and *pbl*². Metaphase, *n* = 46 (WT) and 43 (*pbl*²); anaphase, *n* = 32 (WT) and 36 (*pbl*²); early telophase, *n* = 28 (WT) and 27 (*pbl*²); late telophase, *n* = 27 (WT) and 24 (*pbl*²); and scission, *n* = 53 (WT) and 42 (*pbl*²). (N) Some Pbl-deficient cells form weak furrows that complete invagination (arrow) but fail to maintain the central spindle. (O and P) Magnification of equatorial region in WT (O and O') and *pbl*² (P) cells. O' and P were taken from C' and I', respectively. Furrow and MT structures are labeled in O. Arrowheads and brackets mark the cleavage plane and central spindle, respectively, in O' and P. *pbl*² embryos lack furrow MTs and show a weak central spindle (P). (Q) Percentage of normal (+++), weak (++), and severely disrupted (+) furrow MTs during early telophase in WT and *pbl*². *n* = 41 (WT) and 33 (*pbl*²). (R) Pbl shows punctate localization where furrow MTs contact the leading furrow edge (arrows). Bars, 4 μ m. Error = SEM among embryos.

(Fig. 4, arrows) and midzone MTs condense to form the central spindle (Fig. 8 A, bracket; and Video 8, available at <http://www.jcb.org/cgi/content/full/jcb.200803096/DC1>), which is maintained throughout cytokinesis. In contrast, *pbl*⁵ embryos formed midzone MTs at anaphase but failed to form furrow MTs or maintain a stable central spindle (Fig. 8 B and Video 9). Collectively with the fixed tissue analysis, these data indicate that Pbl-deficient embryos have defects in furrow MT formation, central spindle maintenance, and targeting of vesicles and actin.

Although Pbl is zygotically required for the onset of cytokinesis, the hypomorphic *pbl*⁵ allele produces a range of cytokinesis defects, from cells that fail to initiate furrows to cells with fully invaginated furrows that subsequently regress. We therefore examined *pbl*⁵ embryos for correlations between central spindle formation, furrow invagination, and actin puncta delivery. During mitotic cycle 14 in *pbl*⁵ embryos, a majority of cells lacked a stable central spindle and showed incomplete

furrowing (71 and 71%, respectively; *n* = 24; Fig. 8 C). Cells that lacked a central spindle had severe actin puncta localization defects (Fig. 8 C). Overall, the appearance of the central spindle in *pbl*⁵ embryos ranged from normal to a complete loss of spindle. Actin puncta delivery to the cell equator was correlated to central spindle function: as central spindle organization progressively worsened, actin puncta targeting was further weakened. These observations reveal coordination between central spindle function, furrow ingression, and actin-positive vesicle recruitment. Membrane addition associated with cell size expansion at prophase was normal in *pbl*⁵ embryos (Fig. S2, available at <http://www.jcb.org/cgi/content/full/jcb.200803096/DC1>), indicating that the membrane trafficking phenotype in *pbl*⁵ is not caused by general secretion defects. Collectively, these data indicate that central spindle and furrow MT maintenance is an important factor in actin puncta delivery to the cleavage plane and implicate Pbl in membrane trafficking during cytokinesis.

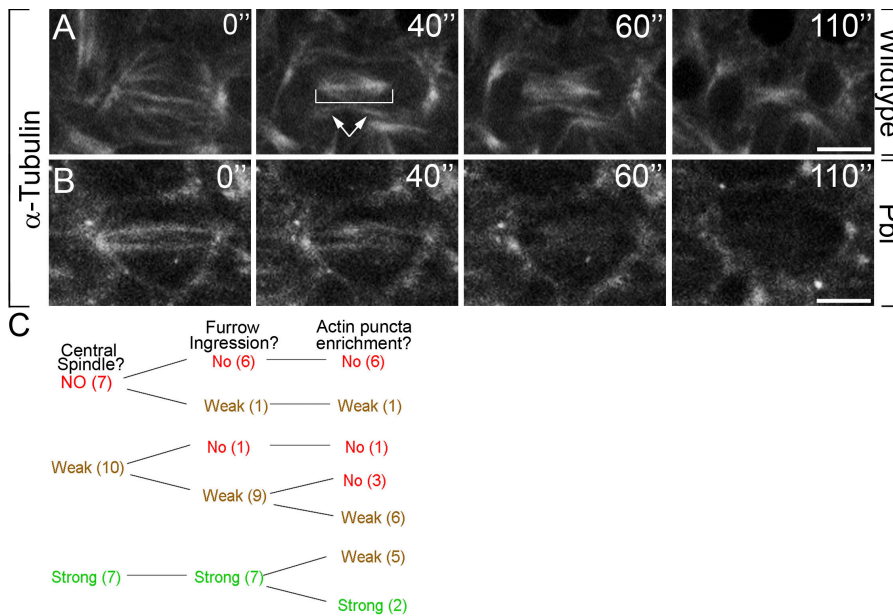


Figure 8. *pbl* embryos show defects in central spindle maintenance, furrow ingression, and vesicle transport. Genotypes are indicated on the right. All images show live embryos. Fluorescent α -tubulin was injected at cellularization. (A) Central spindle and furrow MT formation in WT. Bracket, central spindle; arrows, furrow MTs. (B) Mitotic cells in *pbl*² mutants show mid-zone MTs but lack furrow MTs and a stable central spindle. (C) *pbl*² phenotype ranges from cells that lack a central spindle to cells with a strong central spindle. Central spindle severity (left) correlates with defects in furrow invagination (middle) and actin puncta mislocalization (right). *n* is shown in parenthesis. For full videos, see Videos 8 and 9, available at <http://www.jcb.org/cgi/content/full/jcb.200803096/DC1>. Bars, 5 μ m.

Distinct role of Pbl in production of F-actin puncta and vesicles

In addition to Pbl involvement in furrow MT formation and vesicle targeting, we also find that Pbl function influences the number of vesicles in the cell. Live imaging revealed that a portion of *pbl* mutant cells had a central spindle that appeared normal yet showed reduced actin enrichment at the cell equator (Fig. 8 C). Actin puncta localization and quantity were quantified in *pbl*² mutants to further investigate the role of Pbl in actin puncta targeting and production (Fig. 4 J). Actin puncta distribution, relative to the central spindle, was scored in a 3- μ m-thick section per cell. In both WT and *pbl* mutant cells with normal central spindles, about half the actin puncta localized to central spindle MTs (Fig. 4 J, 47.5 ± 1.9 and $42.5 \pm 6.2\%$, respectively) and half localized to cytoplasmic regions outside of the central spindle. However, *pbl* mutant cells with normal central spindles had a greater than twofold reduction in total number of actin puncta scored per cell (Fig. 4 J, 13.3 ± 1.6 [WT] vs. 5.1 ± 0.59 [*pbl*]). These data indicate that *pbl* mutant cells with normal central spindles maintain vesicle targeting yet have defects in the production and/or maintenance of actin puncta.

Reduced actin puncta in *pbl* mutant cells led us to ask whether the vesicles that normally associate with the actin puncta are also reduced. To address this issue, localization and quantity of Dah-positive vesicles were assayed. In both WT and *pbl* mutant cells with normal central spindles, about two-thirds of Dah-positive vesicles localized to central spindle MT bundles (60.9 ± 1.3 and $57.6 \pm 2.3\%$, respectively; Fig. 4 J). However, *pbl* mutant cells with normal central spindles have about a twofold reduction in the total number Dah-labeled vesicles scored per cell (Fig. 4 J, 11.3 ± 0.48 [WT]; 5.3 ± 0.37 [*pbl*]). Collectively, these data suggest a previously unsuspected role for Pbl in promoting actin puncta and vesicle production.

We next examined if loss of vesicle targeting was due the absence of a central spindle rather than a major reduction in the number of cytoplasmic vesicles. *pbl* mutant cells lacking central

spindles showed a random cytoplasmic distribution for both actin- and Dah-positive vesicles (Fig. 4 J, right graph). Yet, the overall quantity of vesicles was similar among cells, regardless of whether a central spindle was present or absent (Fig. 4 J, 5.1 ± 0.59 and 4.7 ± 0.69 [actin]; 5.3 ± 0.37 and 5.6 ± 0.50 [Dah], respectively). Collectively, these data illustrate that the quantity of vesicles is reduced in all *pbl* mutant cells, but only cells with a central spindle retain the ability to target vesicles to the cell equator.

Discussion

Vesicle recruitment to invaginating furrows

Although it is well established that furrow invagination in animal cytokinesis involves vesicle-mediated membrane addition (Strickland and Burgess, 2004; Albertson et al., 2005; Otegui et al., 2005), little is known about the mechanisms by which vesicles are recruited and targeted to the furrows. Our studies suggest that both recruitment and targeting rely on transport of vesicles along the central spindle and furrow MTs to the leading edge of the cytokinesis furrow.

This pattern of vesicle transport is not specific to cycle 14 mitotic divisions immediately after cellularization in *D. melanogaster*. We observed vesicle accumulation at the cell equator and subsequent enrichment at furrows in several tissue types and developmental stages, including undifferentiated cells in early embryos as well as epithelia and neuroblasts in late stage embryos. In addition, live analysis in Zebrafish reveals that vesicles tagged with the V-Snare Vamp-2-GFP are recruited to the cleavage furrow in an MT-dependent manner during cytokinesis (Li et al., 2006).

Vesicle recruitment during cytokinesis is now thought to be an important source of membrane during furrow invagination (Albertson et al., 2005; Otegui et al., 2005). Yet, it has long been established that the delivery of secretory vesicles to specific membrane sites is necessary for many other cellular functions,

including synapse formation, neurotransmitter exocytosis, and establishment and maintenance of cell polarity (for review see Hsu et al., 1999). For example, polarized epithelial cells use vesicles to selectively deliver transmembrane proteins to apical or basolateral target membrane (Folsch, 2005). These findings raise the possibility that during cytokinesis, vesicles deliver specific proteins required for processes such as contraction, scission, and endocytosis at the furrow. Support for this comes from results indicating that vesicles may deliver cell–cell adhesion components essential for the completion of cytokinesis in Zebrafish (Li et al., 2006). In this paper, we describe vesicle-mediated delivery of a key contractile ring component, F-actin, to furrows during mid-to-late cytokinesis.

Actin localization to cleavage furrows

F-actin concentration at the cleavage furrow may occur through localized polymerization of F-actin or transport of preexisting F-actin to the furrow (Eggert et al., 2006). Support for the former mechanism comes from several studies demonstrating that formin-mediated polymerization of unbranched F-actin filaments at the cleavage furrow play a role in contractile ring formation in several systems (for review see Piekny et al., 2005).

The second mechanism of concentrating F-actin at the cleavage furrow is through transport and targeting of F-actin to the cleavage furrow. Studies in dividing normal rat kidney (NRK) cells indicate that actin concentration at the cleavage furrow involves a redistribution of cortical actin filaments (Cao and Wang, 1990a,b). In this system, fluorescently labeled actin filaments showed uniform cortical localization before initiation of cytokinesis. During early cytokinesis stages, labeled actin filaments became depleted from polar regions and highly enriched at the equatorial cell cortex. Actin filament aggregates appeared to move from polar regions to the cell equator, suggesting that cortical flow promotes F-actin redistribution to the furrows in NRK cells.

MTs may also play a role in F-actin recruitment by facilitating the transport of F-actin toward MT plus ends in the region of furrow formation. In *D. melanogaster*, actin filaments have been shown to move toward MT plus ends (Foe et al., 2000), and 21 proteins have been identified that interact with both actin and MTs (Sisson et al., 2000). Potential motor proteins include the kinesin-like proteins CHO1 and KLP3A, which localize to the spindle midzone and interact with actin (Sisson et al., 2000; Kuriyama et al., 2002). The spindle midzone is also known to effect the distribution of cortical actin. For example, micromanipulations to alter spindle MTs in grasshopper spermatocytes demonstrate that actin filaments continuously redistribute to precisely align with the repositioned central spindle (Alsop and Zhang, 2004).

Other work has suggested a vesicle-mediated mode of actin delivery to ingressing furrows. It has been proposed that in early *D. melanogaster* embryos, the delivery of actin to specialized metaphase furrows is linked to the recycling pathway (Riggs et al., 2003). In this system, the mammalian Arpophilin-2 homologue Nuf functions in concert with the small GTPase Rab11 to organize RE. Reduced protein levels affect membrane and actin organization at metaphase furrows. Actin showed ves-

icle association at this stage, leading to speculation that actin recruitment to metaphase furrows is vesicle based. However, the sources of vesicles that associate with actin remain unidentified. In addition, vesicle-based actin delivery to furrows has been thought to be a mechanism specific to the specialized metaphase furrows of the early *D. melanogaster* embryo. This paper directly addresses these issues by demonstrating that conventional cytokinesis involves a mechanism in which endosome-derived vesicles transport actin to ingressing furrows.

This study supports a model in which preformed F-actin is targeted to ingressing furrows yet does not exclude mechanisms involving formin and ARP2/3-mediated de novo actin filament assembly. Our studies are consistent with previous observations that labeled actin filaments associate with vesicles (Riggs et al., 2003; Fernandez-Borja et al., 2005; Ridley, 2006). In this paper, we further show very strong actin association with endosome-derived vesicles and that these actin-positive vesicles are targeted as a unit to furrows via MTs. Cytoplasmic actin puncta accumulate at central spindle and furrow MTs and appear to move along MT bundles, which is important for actin enrichment at the cell equator during cytokinesis. In particular, actin- and Dah-positive vesicles accrue at the contact point between furrow MTs and the leading furrow edge. In contrast to studies with NRK cells, we do not observe a noticeable decrease in actin intensity at polar regions. These observations further support a model in which a considerable amount of cytoplasmic actin filaments are targeted by a vesicle-based mechanism that utilizes furrow MTs and the central spindle for trafficking. Actin enrichment at furrows peaks during mid-to-late cytokinesis stages, suggesting that this mechanism does not primarily provide an early source of actin for contractile ring assembly but rather a late source of actin. This raises the possibility that furrow-associated actin may have essential roles during late cytokinesis, such as scission or endocytosis. Furthermore, strong actin association with endosome-derived vesicles in the vicinity of invaginating furrows suggests that the recycling pathway not only provides a source of new membrane and actin but also couples and targets their delivery to cytokinesis furrows.

The role of the central spindle in actin and vesicle transport

This paper supports a model in which the central spindle plays an important role in coordinating F-actin and vesicle transport with furrow elongation and scission. Various subpopulations of vesicles accumulate and closely localize at central spindle MT bundles. Loss of the central spindle results in dramatic F-actin and vesicle mislocalization. These data suggest that the central spindle may have a direct role in F-actin and vesicle recruitment, such as providing a scaffold for vesicle transport via a molecular motor.

Support for this model comes from studies showing that molecular motors use the central spindle as a substrate for vesicle transport. Several kinesin-related proteins, including CHO1/MKLP, KLP3A, Rab6-KIFL, and MPP1, localize to the midzone where they promote central spindle formation and stability (Williams et al., 1995; Giansanti et al., 1998; Jantsch-Plunger and Glotzer, 1999; Hill et al., 2000; Matulienė and Kuriyama,

2002; Abaza et al., 2003). RNAi inhibition against mammalian CHO1/MKLP and MPP1, as well as the *C. elegans* CHO1/MKLP homologue Zen4, causes ingressing furrows to regress, indicating that these proteins are important late in cytokinesis (Powers et al., 1998; Raich et al., 1998; Matulienė and Kuriyama, 2002; Abaza et al., 2003). Consistent with a late role in cytokinesis, we find vesicle and actin puncta associating with MT structures during mid-to-late cytokinesis, with the strongest enrichment at late cytokinesis.

In mammalian NRK cells, the kinesin II subunit KIF3B colocalizes with syntaxin-containing vesicles to the central spindle during telophase (Fan and Beck, 2004). Expression of the dominant-negative tail of KIF3B results in a reduction of syntaxin at the central spindle and also causes cytokinesis defects. KIF3B physically interacts with the spectrin Syne-1 and targets Syne-1 to the central spindle, and reduced Syne-1 function has an identical phenotype to KIF3B. Because spectrins interact with membranes, one hypothesis is that spectrins link vesicles to kinesins, which transport the vesicles along the central spindle, facilitating vesicle fusion with each other and the advancing furrow (Fan and Beck, 2004).

A specialized MT population, furrow MTs, promotes F-actin and vesicle addition at ingressing furrows

In addition to the central spindle, a specialized population of furrow MTs that promote cytokinesis has been described in *Xenopus laevis*, Sea Urchin, and Zebrafish blastomeres (Danilchik et al., 1998; Jesuthasan, 1998; Larkin and Danilchik, 1999). In these systems, furrow MTs are derived from midzone MTs, localize to deepening furrows, and orient perpendicular to furrows. Furrow MTs have been hypothesized to play a role in promoting membrane addition to furrows during cell division by directing vesicles to the cytoplasmic bridge (Danilchik et al., 1998; Jesuthasan, 1998; Larkin and Danilchik, 1999). Despite the presence of a normal central spindle, Zebrafish *nebel* mutants showed reduced furrow MTs and reduced membrane deposition at the furrow (Pelegrini et al., 1999). In a reciprocal scenario, *D. melanogaster* embryos expressing a stable cyclin B3 lacked a central spindle but showed MT structures that resembled furrow MTs and were able to form ingressing furrows (Parry and O'Farrell, 2001). Collectively, these reports suggest that furrow MTs are distinct from the central spindle and are important for furrow ingression.

In this paper, we propose that furrow MTs promote F-actin and vesicle recruitment to ingressing furrows during cytokinesis in *D. melanogaster* embryos. Live and fixed imaging show that Dah- and F-actin-associated vesicles concentrate near and move adjacent to furrow MTs. Both 2D and 3D imaging reveal F-actin- and Dah-positive vesicles in close proximity to where furrow MTs intersect with the leading furrow edge and appear to incorporate into the invaginating furrow. In addition, the loss of furrow MTs and the central spindle in *pbl* mutants causes a dramatic mislocalization of all vesicle subpopulations examined. These data support a model in which F-actin and vesicles are delivered as a unit toward ingressing furrows via central spindle and furrow MTs.

Role for Pbl in furrow MT formation and maintenance

Pbl-mediated RhoA signaling at the putative cleavage furrow site plays a key role in contractile ring assembly and subsequent contraction (for review see Piekny et al., 2005). Depletion of Pbl causes furrowing defects and loss of the central spindle (Prokopenko et al., 1999). In addition to these defects, we show in both fixed and living embryos that reduced Pbl function causes early defects in furrow MT formation during mitosis. One explanation for this result is based on the mutual dependence between the contractile ring and central spindle formation. Previous functional studies have shown that obstructing contractile ring assembly and function can reduce central spindle stability (Cao and Wang, 1996; Giansanti et al., 1998; Gatti et al., 2000; Somma et al., 2002). In particular, removing Pbl function by RNAi in S2 cells (Somma et al., 2002) or *pbl* alleles in spermatocytes (Giansanti et al., 2004) causes a loss of the central spindle. Therefore, it may be that this mutual dependence extends to the furrow MTs and, thus, that the loss of Pbl function causes a primary defect in contractile ring formation, which results in a secondary defect in furrow MT organization. However, several of our observations suggest a primary role for Pbl in regulating MT organization. First, a small minority of Pbl-deficient cells formed weak furrows that completed ingression but lacked recognizable furrow MTs. Therefore, in spite of having a contractile ring that is functional enough to promote furrow ingression, these cells have severely disorganized furrow MT bundles, suggesting that Pbl plays a role in organizing these MT structures. Second, Pbl protein colocalized with furrow MTs at the contact point with the leading furrow edge. Third, the *pbl* spindle phenotype does not appear to be simply caused by failed MT maintenance during a prolonged telophase because furrow MT formation is abnormal during early telophase. In particular, one third of *pbl* deficient cells lacked furrow MTs during furrow initiation.

Our results support a model in which components at the leading furrow edge interact with furrow MTs. Furrow MTs would provide the cleavage furrow with structural support as well as a source of vesicle-derived membrane and proteins. The leading edge of the furrow could provide a docking site for vesicle fusion. Contact between the central spindle and furrow MTs may be linked by thin bundles of MTs that appear to connect the two structures. In support of this view, furrow MT defects in *pbl* embryos precede central spindle defects, suggesting that furrow MTs are a distinct MT population and their stability influences central spindle stability.

Furrow-associated components, such as Pbl, could provide cues stimulating furrow MT formation and maintenance. For example, Pbl has been shown to physically interact with RacGAP50c, a protein with MT bundling activity that localizes to cortical MTs adjacent to the future cleavage site during anaphase (Somers and Saint, 2003; Zavortink et al., 2005). Alternatively, Pbl may affect MT stability through Rho signaling. Rho family members are well known for their role in F-actin remodeling and accumulating evidence indicates a role for Rho and formins in regulating MT dynamics (Waller and Alberts, 2003; Narumiya and Yasuda, 2006). In particular, RhoA can

promote selective MT stabilization in NIH3T3 cells (Cook et al., 1998). Furthermore, several studies in mouse fibroblasts and mammalian cell culture suggest that RhoA influences MT organization through its downstream target, the formin Diaphanous (Tominaga et al., 2000; Ishizaki et al., 2001; Kato et al., 2001; Palazzo et al., 2001, 2004; Gasteier et al., 2005). In this paper, we find that the guanine nucleotide exchange factor for RhoA, Pbl, colocalizes with furrow MTs, which is consistent with the idea that spindle MT defects observed in *pbl* embryos are caused by a loss of signaling to downstream effectors such as RhoA and Diaphanous.

Role of Rho signaling in actin and vesicle production and maintenance

Somewhat surprisingly, *pbl* mutant cells have a reduction in the number of actin- and Dah-positive vesicles, revealing *pbl* defects in vesicle production and/or maintenance. One explanation is that vesicle production and/or maintenance is highly sensitive to even subtle abnormalities in furrow composition, central spindle, or furrow MT organization. Alternatively, these data may reveal a new role for Pbl in coordinating vesicle-associated actin dynamics and vesicle traffic during cytokinesis. These findings are in accord with studies in other systems indicating that Pbl could influence vesicle dynamics through its downstream target RhoA and Dia (Lamaze et al., 1996; Qualmann and Mellor, 2003; Fernandez-Borja et al., 2005; Ridley, 2006).

Materials and methods

D. melanogaster stocks

The following stocks were obtained from the Bloomington Stock Center: Syt-GFP, n-Syb-GFP, RhoA-GFP, Rab7-GFP, Rab5-GFP, Grasp65-GFP, Clc-GFP, *pbl*^Δ, and *pbl*^Δ. Each stock is described in the Flybase database (<http://flybase.bio.indiana.edu/>). *pbl*^Δ and *pbl*^Δ are listed as null and hypomorphic alleles, respectively. The following are also included in this study: Dlg-GFP (C. Doe, University of Oregon, Eugene, OR), Tubulin-GFP (T.C. Kaufman, Indiana University, Bloomington, IN), Dah-GFP (T. Hsieh, Duke University Medical Center, Durham, NC), and Maternal-Gal4 V32 (D. St Johnston, Gurdon Institute, Cambridge, UK). Oregon R served as the WT control stock. All stocks were raised at 25° on standard maize meal/molasses media.

Genetics

The following UAS transgenes were expressed using maternal-Gal4 V32 (provided by S. Cambell, University of Alberta, Alberta, Canada): Syt, Dlg, n-Syb, Rab7, Rab5, Grasp65, and Clc-GFP. Dah-GFP and RhoA-GFP were expressed from their normal promoter. Syt-GFP expression in a *pbl*^Δ mutant background involved the following genetics: UAS-Syt-GFP was recombined onto a second chromosome, containing mat-Gal4, using standard genetics. UAS-Syt-GFP, mat-Gal4/UAS-Syt-GFP, mat-Gal4; Dr/TM3,ser flies were generated and crossed to *pbl*^Δ/TM3,ser. UAS-Syt-GFP, mat-Gal4/+; *pbl*^Δ/TM3,ser were selected and self-crossed. Homozygous *pbl*^Δ mutant embryos were selected by the occurrence of cleavage furrow regression and multinucleate cells.

Fixation and immunofluorescence

Embryos were collected and fixed using standard methods (Sullivan et al., 2000). Pebble stains involved methanol + 6% formaldehyde fix for 20 min. Scribble, α -tubulin, and phosphohistone H3 triple stains used 9% fix. Actin was stained with fluorescently labeled Alexa Fluor 488-conjugated phalloidin (Invitrogen) with a methanol-free formaldehyde fix on hand-devitellinized embryos as described in Rothwell et al. (1999). The primary antibodies used include polyclonal rabbit anti-Scribble (1:2,500; Albertson and Doe, 2003), monoclonal mouse anti- α -tubulin (1:200; Sigma-Aldrich), polyclonal rat anti-Pebble (1:1,000; H. Bellen, Baylor College of Medicine, Houston, TX), monoclonal mouse anti- γ -tubulin (1:400; Sigma-Aldrich),

and rabbit anti-phosphohistone H3 (1:1,000; Millipore). The secondary antibodies Cy5-conjugated goat anti-rabbit IgG and Alexa Fluor 594-conjugated goat anti-mouse IgG (Invitrogen) were used at 1:400. Antibodies were applied and embryos mounted as previously described (Sullivan et al., 2000).

Live embryo analysis

Embryos were prepared for microinjection and time-lapse scanning confocal microscopy as previously described (Tram et al., 2001). Reagents, including rhodamine-conjugated tubulin (Invitrogen), FM1-43 dye (Invitrogen), fluorescein-conjugated tubulin (Cytoskeleton, Inc.), and rhodamine non-muscle actin (Cytoskeleton, Inc.), were injected at 30% egg length during mid cellularization.

Microscopy

Microscopy was performed at room temperature using an inverted photo-scope (DMIRB; Leitz) equipped with a scanning laser confocal imaging system (TCS NT; Leica). Images were acquired with a 63 \times lens and confocal software (V2.61; Leica). Confocal images were processed with ImageJ (National Institutes of Health) for whole-image brightness and contrast, and figures were assembled in Photoshop (v9.0; Adobe). Videos were made from datasets containing a single image in the z axis that were collected over time (time intervals specified in figures) and converted into an uncompressed AVI video. 3D imaging in live embryos was conducted on a spinning disc-equipped microscope (Eclipse TE200-E; Nikon). 3D reconstructions were performed on Velocity 4 software (Improvision). Videos were trimmed and cropped in ImageReady (v9.0; Adobe) and converted to QuickTime videos (Apple) using PNG lossless compression.

Vesicle localization quantifications

Dah-GFP and actin-positive vesicle localization was scored relative to the central spindle in a 3- μ m-thick section per cell, which included the depth of the central spindle (Fig. 4). In *pbl* mutant cells that lacked a central spindle, vesicles were scored in the xy plane by their appearance in either the middle third of the cell or in the outer two-thirds of the cell. A 3- μ m-thick z section at cell center depth was scored. Designation of cell center in the z plane (Figs. 2 and 4) was based on the maximum circumference of the cell cortex and nuclei. Designation of the middle one-third region in the xy plane was based on the position of nuclei.

Online supplemental material

Fig. S1 shows that Syt-GFP marks vesicular structures in various cell types and at various developmental time points. Fig. S2 shows plasma membrane expansion during cycle 14 in living WT and *pbl* embryos. Video 1 shows that Syt-GFP tagged vesicles are targeted to cleavage furrows during cytokinesis. Video 2 shows that actin puncta are targeted to ingressing cleavage furrows in WT embryos. Video 3 shows 3D imaging of α -tubulin and actin dynamics in WT embryo. Video 4 shows 3D imaging of α -tubulin and Dah dynamics in WT embryo. Video 5 shows actin and vesicle recruitment to ingressing furrows in WT embryo. Video 6 shows actin and vesicle recruitment to ingressing furrows in Pbl-deficient cell with strong furrowing defect. Video 7 shows actin and vesicle recruitment to ingressing furrows in Pbl-deficient cell with weak furrowing defect. Video 8 shows mitotic spindle dynamics in WT embryo. Video 9 shows mitotic spindle dynamics in *pbl* embryo. Online supplemental material is available at <http://www.jcb.org/cgi/content/full/jcb.200803096/DC1>.

We thank C. Doe, S. Cambell, and H. Bellen for fly stocks and antibodies, L. Serbus and C. Lindley for manuscript comments, and Dustin Updike for technical advice.

This work was supported by a National Institutes of Health postdoctoral fellowship to R. Albertson (GM075670) and a National Institutes of Health grant to W. Sullivan (GM046409). Essential technical support was provided by National Institutes of Health grants to B. Saxton (GM46295) and S. Strome (GM34059).

Submitted: 19 March 2008

Accepted: 29 April 2008

References

- Abaza, A., J.M. Soleilhac, J. Westendorf, M. Piel, I. Crevel, A. Roux, and F. Pirollet. 2003. M phase phosphoprotein 1 is a human plus-end-directed kinesin-related protein required for cytokinesis. *J. Biol. Chem.* 278:27844–27852.

- Albertson, R., and C.Q. Doe. 2003. Dlg, Scrib and Lgl regulate neuroblast cell size and mitotic spindle asymmetry. *Nat. Cell Biol.* 5:166–170.
- Albertson, R., B. Riggs, and W. Sullivan. 2005. Membrane traffic: a driving force in cytokinesis. *Trends Cell Biol.* 15:92–101.
- Alsop, G.B., and D. Zhang. 2004. MTs continuously dictate distribution of actin filaments and positioning of cell cleavage in grasshopper spermatocytes. *J. Cell Sci.* 117:1591–1602.
- Bilder, D., M. Li, and N. Perrimon. 2000. Cooperative regulation of cell polarity and growth by *Drosophila* tumor suppressors. *Science*. 289:113–116.
- Burgess, R.W., D.L. Deitcher, and T.L. Schwarz. 1997. The synaptic protein syntaxin1 is required for cellularization of *Drosophila* embryos. *J. Cell Biol.* 138:861–875.
- Cao, L.G., and Y.L. Wang. 1990a. Mechanism of the formation of contractile ring in dividing cultured animal cells. I. Recruitment of preexisting actin filaments into the cleavage furrow. *J. Cell Biol.* 110:1089–1095.
- Cao, L.G., and Y.L. Wang. 1990b. Mechanism of the formation of contractile ring in dividing cultured animal cells. II. Cortical movement of microinjected actin filaments. *J. Cell Biol.* 111:1905–1911.
- Cao, L.G., and Y.L. Wang. 1996. Signals from the spindle midzone are required for the stimulation of cytokinesis in cultured epithelial cells. *Mol. Biol. Cell.* 7:225–232.
- Cook, T.A., T. Nagasaki, and G.G. Gundersen. 1998. Rho guanosine triphosphatase mediates the selective stabilization of MTs induced by lysophosphatidic acid. *J. Cell Biol.* 141:175–185.
- D'Avino, P.P., M.S. Savoian, and D.M. Glover. 2005. Cleavage furrow formation and ingression during animal cytokinesis: a microtubule legacy. *J. Cell Sci.* 118:1549–1558.
- Danilchik, M.V., W.C. Funk, E.E. Brown, and K. Larkin. 1998. Requirement for MTs in new membrane formation during cytokinesis of *Xenopus* embryos. *Dev. Biol.* 194:47–60.
- Deitcher, D.L., A. Ueda, B.A. Stewart, R.W. Burgess, Y. Kidokoro, and T.L. Schwarz. 1998. Distinct requirements for evoked and spontaneous release of neurotransmitter are revealed by mutations in the *Drosophila* gene neuronal-synaptobrevin. *J. Neurosci.* 18:2028–2039.
- Echard, A., and P.H. O'Farrell. 2003. The degradation of two mitotic cyclins contributes to the timing of cytokinesis. *Curr. Biol.* 13:373–383.
- Echard, A., G.R. Hickson, E. Foley, and P.H. O'Farrell. 2004. Terminal cytokinesis events uncovered after an RNAi screen. *Curr. Biol.* 14:1685–1693.
- Eggert, U.S., A.A. Kiger, C. Richter, Z.E. Perlman, N. Perrimon, T.J. Mitchison, and C.M. Field. 2004. Parallel chemical genetic and genome-wide RNAi screens identify cytokinesis inhibitors and targets. *PLoS Biol.* 2:e379.
- Eggert, U.S., T.J. Mitchison, and C.M. Field. 2006. Animal cytokinesis: from parts list to mechanisms. *Annu. Rev. Biochem.* 75:543–566.
- Estes, P.S., G.L. Ho, R. Narayanan, and M. Ramaswami. 2000. Synaptic localization and restricted diffusion of a *Drosophila* neuronal synaptobrevin–green fluorescent protein chimera in vivo. *J. Neurogenet.* 13:233–255.
- Fan, J., and K.A. Beck. 2004. A role for the spectrin superfamily member Syne-1 and kinesin II in cytokinesis. *J. Cell Sci.* 117:619–629.
- Fernandez-Borja, M., L. Janssen, D. Verwoerd, P. Hordijk, and J. Neefjes. 2005. RhoB regulates endosome transport by promoting actin assembly on endosomal membranes through Dia1. *J. Cell Sci.* 118:2661–2670.
- Finger, F.P., and J.G. White. 2002. Fusion and fission: Membrane trafficking in animal cytokinesis. *Cell*. 108:727–730.
- Foe, V.E. 1989. Mitotic domains reveal early commitment of cells in *Drosophila* embryos. *Development*. 107:1–22.
- Foe, V.E., C.M. Field, and G.M. Odell. 2000. MTs and mitotic cycle phase modulate spatiotemporal distributions of F-actin and myosin II in *Drosophila* syncytial blastoderm embryos. *Development*. 127:1767–1787.
- Folsch, H. 2005. The building blocks for basolateral vesicles in polarized epithelial cells. *Trends Cell Biol.* 15:222–228.
- Gasteier, J.E., S. Schroeder, W. Muranyi, R. Madrid, S. Benichou, and O.T. Fackler. 2005. FHOD1 coordinates actin filament and microtubule alignment to mediate cell elongation. *Exp. Cell Res.* 306:192–202.
- Gatti, M., M.G. Giansanti, and S. Bonaccorsi. 2000. Relationships between the central spindle and the contractile ring during cytokinesis in animal cells. *Microsc. Res. Tech.* 49:202–208.
- Giansanti, M.G., S. Bonaccorsi, B. Williams, E.V. Williams, C. Santolamazza, M.L. Goldberg, and M. Gatti. 1998. Cooperative interactions between the central spindle and the contractile ring during *Drosophila* cytokinesis. *Genes Dev.* 12:396–410.
- Giansanti, M.G., R.M. Farkas, S. Bonaccorsi, D.L. Lindsley, B.T. Wakimoto, M.T. Fuller, and M. Gatti. 2004. Genetic dissection of meiotic cytokinesis in *Drosophila* males. *Mol. Biol. Cell.* 15:2509–2522.
- Hill, E., N. Clarke, and F.A. Barr. 2000. The Rab6-binding kinesin, Rab6-KIFL, is required for cytokinesis. *EMBO J.* 19:5711–5719.
- Hime, G., and R. Saint. 1992. Zygotic expression of the pebble locus is required for cytokinesis during the postblastoderm mitoses of *Drosophila*. *Development*. 114:165–171.
- Hsu, S.C., C.D. Hazuka, D.L. Foletti, and R.H. Scheller. 1999. Targeting vesicles to specific sites on the plasma membrane: the role of the sec6/8 complex. *Trends Cell Biol.* 9:150–153.
- Ishizaki, T., Y. Morishima, M. Okamoto, T. Furuyashiki, T. Kato, and S. Narumiya. 2001. Coordination of MTs and the actin cytoskeleton by the Rho effector mDia1. *Nat. Cell Biol.* 3:8–14.
- Jantsch-Plunger, V., and M. Glotzer. 1999. Depletion of syntaxins in the early *Caenorhabditis elegans* embryo reveals a pole for membrane fusion events in cytokinesis. *Curr. Biol.* 9:738–745.
- Jesuthasan, S. 1998. Furrow-associated microtubule arrays are required for the cohesion of zebrafish blastomeres following cytokinesis. *J. Cell Sci.* 111:3695–3703.
- Kato, T., N. Watanabe, Y. Morishima, A. Fujita, T. Ishizaki, and S. Narumiya. 2001. Localization of a mammalian homolog of diaphanous, mDia1, to the mitotic spindle in HeLa cells. *J. Cell Sci.* 114:775–784.
- Kuriyama, R., C. Gustus, Y. Terada, Y. Uetake, and J. Matulienė. 2002. CHO1, a mammalian kinesin-like protein, interacts with F-actin and is involved in the terminal phase of cytokinesis. *J. Cell Biol.* 156:783–790.
- Lamaze, C., T.H. Chuang, L.J. Terlecky, G.M. Bokoch, and S.L. Schmid. 1996. Regulation of receptor-mediated endocytosis by Rho and Rac. *Nature*. 382:177–179.
- Larkin, K., and M.V. Danilchik. 1999. MTs are required for completion of cytokinesis in sea urchin eggs. *Dev. Biol.* 214:215–226.
- Lehner, C.F. 1992. The pebble gene is required for cytokinesis in *Drosophila*. *J. Cell Sci.* 103:1021–1030.
- Li, W.M., S.E. Webb, K.W. Lee, and A.L. Miller. 2006. Recruitment and SNARE-mediated fusion of vesicles in furrow membrane remodeling during cytokinesis in zebrafish embryos. *Exp. Cell Res.* 312:3260–3275.
- Logan, M.R., and C.A. Mandato. 2006. Regulation of the actin cytoskeleton by PIP2 in cytokinesis. *Biol. Cell.* 98:377–388.
- Matulienė, J., and R. Kuriyama. 2002. Kinesin-like protein CHO1 is required for the formation of midbody matrix and the completion of cytokinesis in mammalian cells. *Mol. Biol. Cell.* 13:1832–1845.
- Morita, K., K. Hirono, and M. Han. 2005. The *Caenorhabditis elegans* ect-2 RhoGEF gene regulates cytokinesis and migration of epidermal P cells. *EMBO Rep.* 6:1163–1168.
- Narumiya, S., and S. Yasuda. 2006. Rho GTPases in animal cell mitosis. *Curr. Opin. Cell Biol.* 18:199–205.
- Otegui, M.S., K.J. Verbrugghe, and A.R. Skop. 2005. Midbodies and phragmoplasts: analogous structures involved in cytokinesis. *Trends Cell Biol.* 15:404–413.
- Palazzo, A.F., T.A. Cook, A.S. Alberts, and G.G. Gundersen. 2001. mDia mediates Rho-regulated formation and orientation of stable MTs. *Nat. Cell Biol.* 3:723–729.
- Palazzo, A.F., C.H. Eng, D.D. Schlaepfer, E.E. Marcantonio, and G.G. Gundersen. 2004. Localized stabilization of MTs by integrin- and FAK-facilitated Rho signaling. *Science*. 303:836–839.
- Parry, D.H., and P.H. O'Farrell. 2001. The schedule of destruction of three mitotic cyclins can dictate the timing of events during exit from mitosis. *Curr. Biol.* 11:671–683.
- Pelegri, F., H. Knaut, H.M. Maischein, S. Schulte-Merker, and C. Nusslein-Volhard. 1999. A mutation in the zebrafish maternal-effect gene *nebel* affects furrow formation and vasa RNA localization. *Curr. Biol.* 9:1431–1440.
- Piekny, A., M. Werner, and M. Glotzer. 2005. Cytokinesis: welcome to the Rho zone. *Trends Cell Biol.* 15:651–658.
- Powers, J., O. Bossinger, D. Rose, S. Strome, and W. Saxton. 1998. A nematode kinesin required for cleavage furrow advancement. *Curr. Biol.* 8:1133–1136.
- Prokopenko, S.N., A. Brumby, L. O'Keefe, L. Prior, Y.C. He, R. Saint, and H.J. Bellen. 1999. A putative exchange factor for Rho1 GTPase is required for initiation of cytokinesis in *Drosophila*. *Genes Dev.* 13:2301–2314.
- Qualmann, B., and H. Mellor. 2003. Regulation of endocytic traffic by Rho GTPases. *Biochem. J.* 371:233–241.
- Raich, W.B., A.N. Moran, J.H. Rothman, and J. Hardin. 1998. Cytokinesis and midzone microtubule organization in *Caenorhabditis elegans* require the kinesin-like protein ZEN-4. *Mol. Biol. Cell.* 9:2037–2049.
- Ridley, A.J. 2006. Rho GTPases and actin dynamics in membrane protrusions and vesicle trafficking. *Trends Cell Biol.* 16:522–529.
- Riggs, B., W. Rothwell, S. Mische, G.R.X. Hickson, J. Matheson, T.S. Hays, G.W. Gould, and W. Sullivan. 2003. Actin cytoskeleton remodeling during early *Drosophila* furrow formation requires recycling endosomal components Nuclear-fallout and Rab11. *J. Cell Biol.* 163:143–154.

- Rothwell, W.F., C.X. Zhang, C. Zelano, T.S. Hsieh, and W. Sullivan. 1999. The *Drosophila* centrosomal protein Nuf is required for recruiting Dah, a membrane associated protein, to furrows in the early embryo. *J. Cell Sci.* 112:2885–2893.
- Schweitzer, J.K., and C. D'Souza-Schorey. 2004. Finishing the job: cytoskeletal and membrane events bring cytokinesis to an end. *Exp. Cell Res.* 295:1–8.
- Sisson, J.C., C. Field, R. Ventura, A. Royou, and W. Sullivan. 2000. Lava lamp, a novel peripheral Golgi protein, is required for *Drosophila melanogaster* cellularization. *J. Cell Biol.* 151:905–917.
- Skop, A.R., D. Bergmann, W.A. Mohler, and J.G. White. 2001. Completion of cytokinesis in *C. elegans* requires a brefeldin A-sensitive membrane accumulation at the cleavage furrow apex. *Curr. Biol.* 11:735–746.
- Skop, A.R., H. Liu, J. Yates III, B.J. Meyer, and R. Heald. 2004. Dissection of the mammalian midbody proteome reveals conserved cytokinesis mechanisms. *Science*. 305:61–66.
- Somers, W.G., and R. Saint. 2003. A RhoGEF and Rho family GTPase-activating protein complex links the contractile ring to cortical MTs at the onset of cytokinesis. *Dev. Cell.* 4:29–39.
- Somma, M.P., B. Fasulo, G. Cenci, E. Cundari, and M. Gatti. 2002. Molecular dissection of cytokinesis by RNA interference in *Drosophila* cultured cells. *Mol. Biol. Cell.* 13:2448–2460.
- Strickland, L.I., and D.R. Burgess. 2004. Pathways for membrane trafficking during cytokinesis. *Trends Cell Biol.* 14:115–118.
- Sullivan, W., M. Ashburner, and R.S. Hawley. 2000. *Drosophila* protocols. Cold Spring Harbor Laboratory Press, Cold Spring Harbor, N.Y. 697 pp.
- Tatsumoto, T., X.Z. Xie, R. Blumenthal, I. Okamoto, and T. Miki. 1999. Human ECT2 is an exchange factor for Rho GTPases, phosphorylated in G2/M phases, and involved in cytokinesis. *J. Cell Biol.* 147:921–927.
- Tominaga, T., E. Sahai, P. Chardin, F. McCormick, S.A. Courtneidge, and A.S. Alberts. 2000. Diaphanous-related formins bridge Rho GTPase and Src tyrosine kinase signaling. *Mol. Cell.* 5:13–25.
- Tram, U., B. Riggs, C. Koyama, A. Debec, and W. Sullivan. 2001. Methods for the study of centrosomes in *Drosophila* during embryogenesis. *Methods Cell Biol.* 67:113–123.
- Tucker, W.C., and E.R. Chapman. 2002. Role of synaptotagmin in Ca^{2+} -triggered exocytosis. *Biochem. J.* 366:1–13.
- Waller, B.J., and A.S. Alberts. 2003. The formins: active scaffolds that remodel the cytoskeleton. *Trends Cell Biol.* 13:435–446.
- Williams, B.C., M.F. Riedy, E.V. Williams, M. Gatti, and M.L. Goldberg. 1995. The *Drosophila* kinesin-like protein KLP3A is a midbody component required for central spindle assembly and initiation of cytokinesis. *J. Cell Biol.* 129:709–723.
- Wilson, G.M., A.B. Fielding, G.C. Simon, X. Yu, P.D. Andrews, R.S. Hames, A.M. Frey, A.A. Peden, G.W. Gould, and R. Prekeris. 2005. The FIP3-Rab11 protein complex regulates recycling endosome targeting to the cleavage furrow during late cytokinesis. *Mol. Biol. Cell.* 16:849–860.
- Zavortink, M., N. Contreras, T. Addy, A. Bejsovec, and R. Saint. 2005. Tum/RacGAP50C provides a critical link between anaphase MTs and the assembly of the contractile ring in *Drosophila melanogaster*. *J. Cell Sci.* 118:5381–5392.
- Zhang, Y.Q., C.K. Rodesch, and K. Broadie. 2002. Living synaptic vesicle marker: synaptotagmin-GFP. *Genesis*. 34:142–145.